# Supplementary information

# Digital maps burn huge carbon

**Table of Contents**

## 1. Supplementary Tables

Table S1. Estimating the display energy consumption of the top five public-facing maps in 2021.

| Mobile Map App | User Count | Average Use Time per User (hours) | Average Displaying Energy (Watts) | Displaying Energy Consumption (kWh) |
|---|---|---|---|---|
| Google Maps | 1,000,000,000 | 30.4 | 26.5 | 805,600,000 |
| Amap | 729,500,000 | 70.2 | 27.2 | 1,392,936,480 |
| Baidu Maps | 520,770,000 | 56.4 | 26.6 | 781,279,985 |
| Waze | 150,000,000 | 53.8 | 28.6 | 230,549,760 |
| Tencent Maps | 39,460,000 | 16.8 | 28.1 | 18,628,277 |
| **Total** | **2,439,730,000** | **N/A** | **N/A** | **3,228,994,502** |

Table S2. Estimating the display energy consumption of domain-specific maps in 2021.

| User Type | User Count | Average Use Time per User (kWh) | Displaying Energy Consumption (kWh) |
|---|---|---|---|
| Enterprise | 7,050,902 | 1,625 | 1,005,987,489 |
| Personal | 37,940,379 | 750~1,500 | 2,165,447,131~4,330,894,262 |
| **Total** | **44,991,281** | **N/A** | **3,171,434,620~5,336,881,751** |

Table S3. Nations ranked by residential electricity consumption.

| Rank | Country | Residential Electricity Energy Consumption (kWh) |
|---|---|---|
| 1 | United States | 1,480,803,429,580 |
| 2 | China | 1,139,462,595,520 |
| 3 | India | 301,226,499,300 |
| 4 | Japan | 264,542,802,801 |
| 5 | Canada | 176,390,000,000 |
| 6 | Russia | 163,445,085,162 |
| 7 | France | 161,484,724,800 |
| 8 | Brazil | 149,800,000,000 |
| 9 | Saudi Arabia | 142,480,000,000 |
| 10 | Germany | 127,034,284,317 |
| 11 | Indonesia | 120,151,191,680 |
| 12 | United Kingdom | 107,860,442,782 |
| 13 | Mexico | 75,660,000,000 |
| 14 | Spain | 73,229,685,672 |
| 15 | Korea | 72,020,000,000 |
| 16 | Turkey | 68,160,000,000 |
| 17 | Italy | 66,203,237,520 |
| 18 | Egypt | 62,650,000,000 |

| | | |
|---|---|---|
| 19 | Australia | 60,493,280,934 |
| 20 | United Arab Emirates | 56,400,000,000 |
| 21 | Norway | 49,530,000,000 |
| 22 | Argentina | 47,730,000,000 |
| 23 | South Africa | 46,354,373,066 |
| 24 | Sweden | 44,540,000,000 |
| 25 | Kuwait | 42,732,600,000 |
| 26 | Philippines | 34,282,539,868 |
| 27 | Malaysia | 31,979,874,272 |
| 28 | Poland | 31,400,000,000 |
| 29 | Ukraine | 29,352,908,000 |
| 30 | Netherlands | 24,646,427,540 |
| 31 | Finland | 22,041,000,000 |
| 32 | Algeria | 21,600,000,000 |
| 33 | Qatar | 21,150,000,000 |
| 34 | Switzerland | 20,300,000,000 |
| 35 | Belgium | 19,090,000,000 |
| 36 | Iran | 18,339,000,000 |
| 37 | Nigeria | 16,820,000,000 |
| 38 | Greece | 16,640,000,000 |
| 39 | Czech Republic | 15,420,638,438 |
| 40 | Portugal | 14,065,000,000 |
| 41 | Romania | 14,000,000,000 |
| 42 | New Zealand | 12,876,325,396 |
| 43 | Hungary | 12,760,000,000 |
| 44 | Serbia | 12,115,200,000 |
| 45 | Bulgaria | 11,324,000,000 |
| 46 | Morocco | 11,006,820,000 |
| 47 | Croatia | 10,920,000,000 |
| 48 | Denmark | 10,850,000,000 |
| 49 | Austria | 9,520,000,000 |
| 50 | Ireland | 8,738,816,397 |
| 51 | Slovakia | 6,360,000,000 |
| 52 | Slovenia | 3,808,000,000 |
| 53 | Lithuania | 3,360,000,000 |
| 54 | Estonia | 2,106,000,000 |
| 55 | Latvia | 1,794,000,000 |
| 56 | Cyprus | 1,604,357,000 |
| 57 | Luxembourg | 842,710,000 |
| 58 | Malta | 793,051,776 |

**Data source:**

S1. Goal 13:Take urgent action to combat climate change and its impacts. UN (3 Dec emeber 2022); https://www.un.org/sustainabledevelopment/climate-change

S2. Maps and Sustainable Development Goals. Icaci (4 Decemeber 2022); https://icaci.org/%20maps-and-sustainable-development-goals
S3. Ritchie, H., Roser, M. & Rosado, P. Energy. Ourworldindata (3 Decemeber 2022); https://ourworldindata.org/energy
S4. Ross, A. & Christie, L. Energy Consumption of ICT. UK Parliament (20 Novemb er 2022); https://post.parliament.uk/research-briefings/post-pn-0677/
S5. Waze Statistics and Facts. Expandedramblings (2 Decemeber 2022); https://expandedramblings.com/index.php/waze-statistics-facts/
S6. Russell, E. 9 things to know about Google's maps data: Beyond the Map. Google Cloud (2 Decemeber 2022); https://cloud.google.com/blog/products/maps-platform/9-things-know-about-googles-maps-data-beyond-map
S7. Number of monthly active user number (MAU) of the leading map navigation ap ps in China in September 2022. Statista (5 Decemeber 2022); https://www.statista.com/statistics/1212017/china-leading-map-apps-based-on-monthly-active-users/
S8. China Mobile Internet Industry Development Analysis Report for the First Half of 2019. Sohu (4 Decemeber 2022); https://www.sohu.com/a/329266838_595294
S9. The truth about the power consumption of LED walls. Barco (3 Decemeber 2022); https://www.barco.com/en/news/2020-04-15-ledtalks-truth-about-power-consumption
S10. New Report: Computer Energy Use Can Easily Be Cut in Half. Nrdc (3 Deceme ber 2022); https://www.nrdc.org/experts/pierre-delforge/new-report-computer-energy-use-can-easily-be-cut-half
S11. Power Conservation. Sites Google (5 Decemeber 2022); https://sites.google.com/site/greenersolutionsnow/energy
S12. Greenhouse gas emissions in the ICT sector. Unepccc (1 Decemeber 2022); https://c2e2.unepccc.org/wp-content/uploads/sites/3/2020/03/greenhouse-gas-emissions-in-the-ict-sector.pdf
S13. Introduction to GIS. Evergreen (2 Decemeber 2022); https://www.evergreen.edu/sites/default/files/MPA%20Fall%202020%20Ruth%20IntroGIS%20Elective%20Syllabus%20-%20Update%2009.24.20.pdf
S14. ENVS2364-Introduction to Geographic Information Science. Unitguides (2 Deceme ber 2022); https://unitguides.mq.edu.au/unit_offerings/123549/unit_guide
S15. GIS Certificate | MSU onGEO. Ongeo (2 Decemeber 2022); https://ongeo.msu.edu/certificates/
S16. Geographic Information Systems. Handbooks (3 Decemeber 2022); https://handbooks.uwa.edu.au/unitdetails?code=GEOG2201
S17. Welcome to GIS Development. Mycourses (3 Decemeber 2022); https://mycourses.aalto.fi/course/view.php?id=32866
S18. GIS for Community Development. Pdx (1 Decemeber 2022); https://www.pdx.edu/urban-studies-planning/sites/g/files/znldhr1926/files/2022-02/Amiri%20Syllabus%20USP%20452-001%20GIS%20for%20Community%20Development%20fall%202021.pdf
S19. Higher Education. Worldbank (5 Decemeber 2022); https://www.worldbank.org/en/topic/tertiaryeducation#1
S20. Back-to-school statistics. Nces (4 Decemeber 2022); https://nces.ed.gov/fastfacts/display.asp?id=372

S21. Learning with GIS. Esri (5 Decemeber 2022); https://www.esri.com/news/arcuser/0700/umbrella11.html
S22. Key Dates for Fall and Spring. Coursera (3 Decemeber 2022); https://www.coursera.org/articles/when-does-college-start
S23. Market Share of ESRI. Slintel (3 Decemeber 2022); https://www.slintel.com/tech/mapping-and-gis/esri-market-share#:~:text=The%20top%20three%20of%20ESRI's,Online%20with%2018.45%25%20market%20share
S24. ArcGIS-User-Seminar-2020-Amplify-Your-GIS. Esri (1 Decemeber 2022); https://community.esri.com/t5/arcgis-user-seminar-and-workshop-documents/arcgis-user-seminar-2020-amplify-your-gis-pdf/ta-p/916492?attachment-id=18148
S25. Georgia Power Employee Reviews for GIS Technician. Indeed (2 Decemeber 2022); https://www.indeed.com/cmp/Georgia-Power/reviews?fjobtitle=GIS+Technician
S26. Questions and Answers about GIS Working Hours. Indeed (2 Decemeber 2022); https://www.indeed.com/cmp/GIS/faq/working-hours
S27. Geographical and Sustainability Sciences. Clas (1 Decemeber 2022); https://clas.uiowa.edu/geography/gis-technician-entry-level-minneapolis-mn
S28. Global PC shipments. Canalys (1 Decemeber 2022); https://www.canalys.com/newsroom/global-pc-market-Q4-2021
S29. Geographic Information System (GIS). Enlyft (2 Decemeber 2022); https://enlyft.com/tech/products/esri
S30. Esri Company News. Comparably (2 Decemeber 2022); https://www.comparably.com/companies/esri
S31. More Than 1,000 Employees and Hundreds of Millions of Data. Jumpstory (2 Decemeber 2022); https://jumpstory.com/blog/more-than-thousand-employees-and-hundreds-of-millions-of-data/
S32. Higher Education. Worldbank (4 Decemeber 2022); https://www.worldbank.org/en/topic/tertiaryeducation#1
S33. Digital Map Market Share, Size, Trends, Industry Analysis Report. Polaris Market Research (27 March 2023); https://www.polarismarketresearch.com/industry-analysis/digital-map-market
S34. How Much Time Do You Spend in Front of a Screen. Professionalvisioncareinc (27 December 2022); https://www.professionalvisioncareinc.com/2021/10/11/how-much-time-do-you-spend-in-front-of-a-screen/
S35. Iea. (29 March 2023); https://www.iea.org/
S36. Average Household Electricity Consumption–2023. Shrink That Footprint (29 March 2023); https://shrinkthatfootprint.com/average-household-electricity-consumption/
S37. Statistics Norway. (29 March 2023); https://www.ssb.no/435431/energy-consumption-in-households-in-norway.gwh-kwh
S38. Energy consumption in households by energy source in 2020, GWh. Statistics Finland (29 March 2023); https://www.stat.fi/til/asen/2020/asen_2020_2021-12-16_tau_002_en.html
S39. Energy Consumption in households in republic of serbia. Belgrade (29 March 2023); https://www.stat.gov.rs/media/345275/energy-consumption-in-households-in-republic-of-serbia-2020.pdf

S40. Switzerland Energy Information. Enerdata (29 March 2023); https://www.enerdata.net/estore/energy-market/switzerland/
S41. Poland Energy Information. Enerdata (29 March 2023); https://www.enerdata.net/estore/energy-market/poland/
S42. Residential electricity consumption in Brazil from 2013 to 2021. Statista (29 March 2023); https://www.statista.com/statistics/985975/brazil-residential-electricity-consumption/
S43. Iran Electricity Consumption: Household. CEIC (29 March 2023); https://www.ceicdata.com/en/iran/electricity-generation-and-consumption/electricity-consumption-household
S44. Saudi Arabia's electricity consumption rises 4.2% in 2021. Argaam (29 March 2023); https://www.argaam.com/en/article/articledetail/id/1611319
S45. Energy profile. IRENA (29 March 2023); https://www.irena.org/-/media/Files/IRENA/Agency/Statistics/Statistical_Profiles/Europe/Ukraine_Europe_RE_SP.pdf
S46. Kuwait - Electricity consumption. Countryeconomy.com (29 March 2023); https://countryeconomy.com/energy-and-environment/electricity-consumption/kuwait

**2. Supplementary Figures**

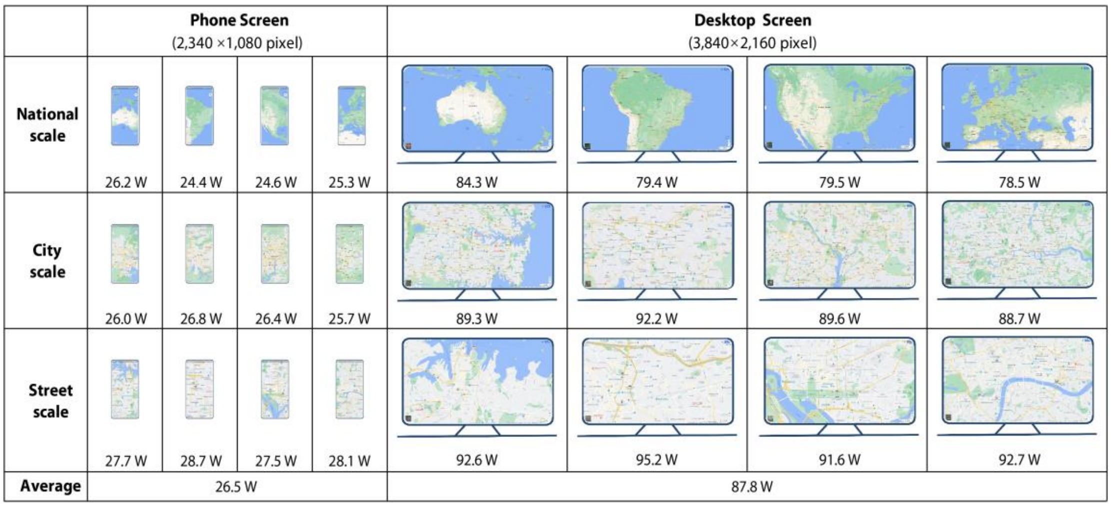


Fig. S1. Estimating the power consumption of Google Maps on both mobile and desktop screens.

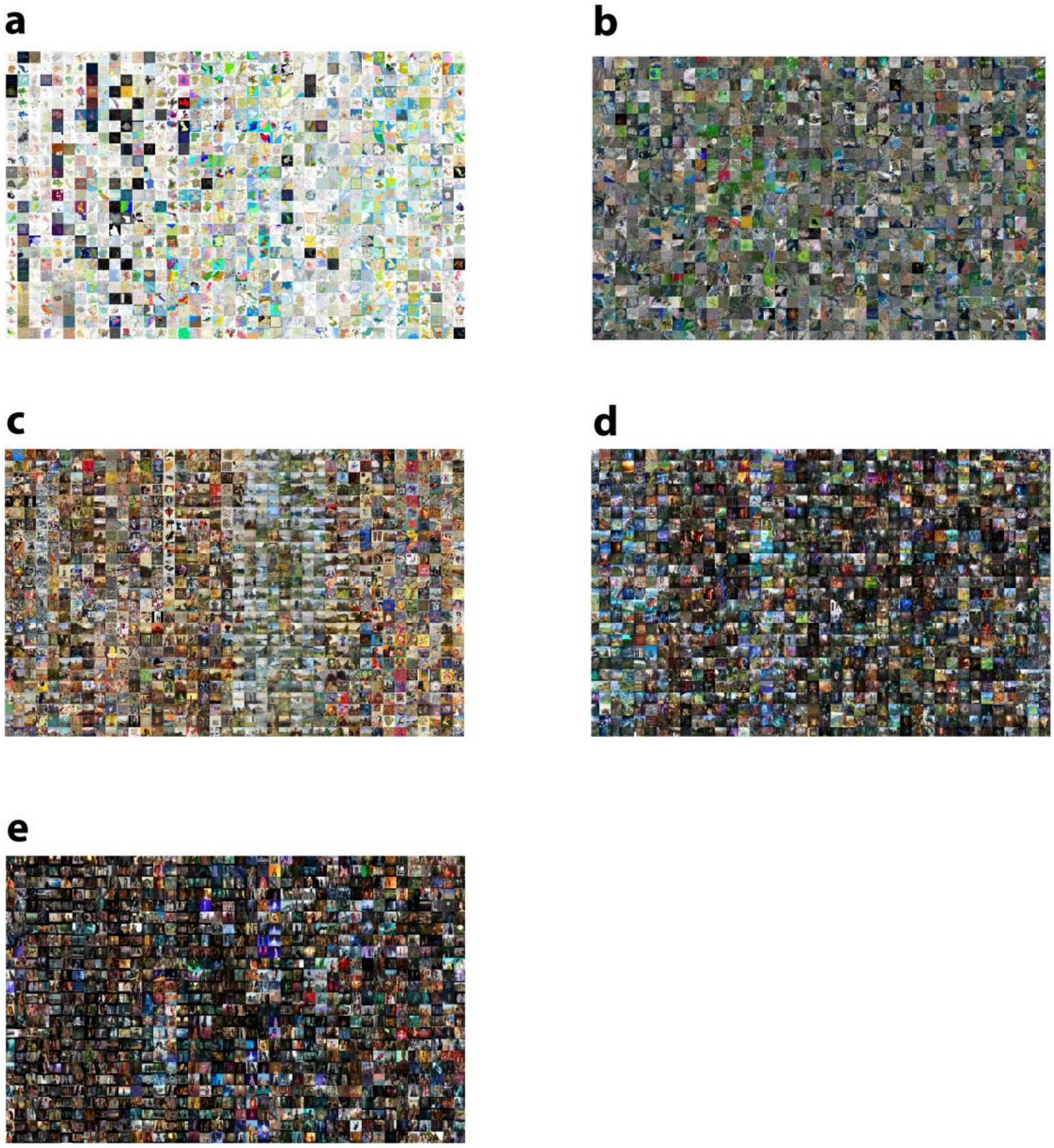


Fig. S2. Overview of the image samples. **a**, Maps. **b**, Remote sensing images. **c**, Paintings. **d**, Video game screenshots. **e**, Movie screenshots.

## 3. Detailed Method Description

### *3.1 Method overview*

As depicted in Fig. S3, we propose a two-step method to reduce the display energy consumed by digital maps. In the first step, we extract the *figure-ground* relationship and three types of semantic relationships (e.g., *differentiation*, *association*, and *order*) that are color-related. Additionally, we quantify the quality of the encoding of the *figure-ground* and semantic relationships, providing a quantitative measure of how well these relationships are represented throughout the map.

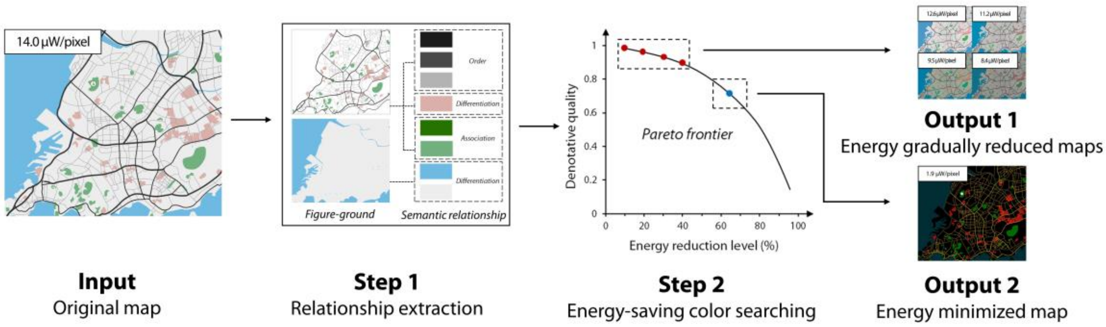


Fig. S3. Overview of our two-step energy-saving method for digital maps.

In the second step, we adopt an iterative approach to replace high-energy colors with low-energy colors, thereby reducing the map's overall energy consumption. To address this energy-saving problem, we introduce an energy estimation model and formulate it as a dual-objective optimization problem: maximizing energy reduction while preserving cartographic quality. We design two energy-saving strategies:

1) Local searching with color shifting consideration: this strategy aims to find a series of color designs that achieve different levels of energy reduction (e.g., 15% or 30%).

2) Global searching with reversed *figure-ground* initiation: this strategy involves searching for a color design that minimizes the map's energy consumption.

By replacing the original color design with the searched color solution, we can obtain an energy-minimized map or a series of energy-gradually reduced maps.

### *3.2 Step 1: Extract figure-ground and semantic relationships*

#### *3.2.1 Parse figure-ground and semantic relationships*

In general, it is crucial to emphasize important map elements as *figures* and distinguish them from the *ground*. Both *figure* and *ground* can be semantically differentiated. In this context, we consider the *figure-ground* relationship as a container for semantic relationships. Specifically, we focus on three types of semantic relationships among map themes: *differentiation*, *association,* and *order*. The *differentiation* relationship employs significant color distance to encode semantic distinctions between two themes. For example, different colors may be used to represent a river and grass. The *association* relationship, by contrast, represents similar semantics using closely related colors. For instance, colors for a lake and ocean may be chosen to convey their shared characteristics. The *order* relationship conveys a sense of gradient or hierarchy through smooth transitions of saturation and/or brightness. This can be seen in the representation of elevation levels of terrain.

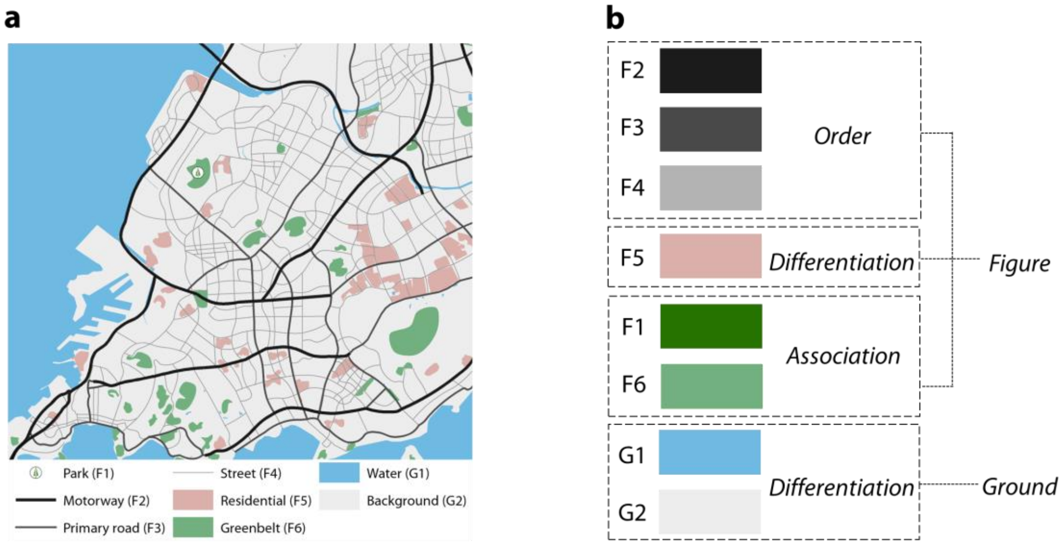


Fig. S4. Illustration of *figure-ground* and semantic relationships of a city map. **a**, An example city map with eight themes, including a background. **b**, The parsed *figure-ground* and semantic relationships.

To illustrate these concepts, we refer to the city map shown in Fig. S4a. In this map, there are eight themes: park, motorway, primary road, street, residential, greenbelt, water, and background. The first six themes are emphasized as *figures*, while water and the background are considered as *grounds*. By parsing the feature layer and analyzing the feature attributes, we can extract detailed semantic relationships. Fig. S4b presents the extracted relationships for this map. For example, park and greenbelt exhibit an *association* relationship, while motorway, primary road, and street display an *order* relationship. There is also a *differentiation* relationship between the residential and the greenbelt. Importantly, in this map, water can be emphasized as a *figure*, and the street can be deemphasized as the *ground*, representing an alternative design decision. However, for the purpose of demonstrating the parsing of *figure-ground* and semantic relationships, we focus on the water-as-*ground* design choice in this example.

Notably, our method supports various design decisions, including water-as-*figure*, which will be further discussed in the next section.

*3.2.2 Quantify figure-ground and semantic relationships*

We aim to quantify how effectively colors are used to encode *figure-ground* and semantic relationships. Colors serve as symbols in two ways: denotative (explicitly conveying qualitative and/or quantitative information) and connotative (implicitly representing concepts or emotions related to mapping themes). As the connotative aspect can be subtle or hidden, our focus is on quantifying denotation, which we refer to as denotative quality.

To assess the denotative quality, we employ color distance as a fundamental indicator for determining semantic relationships. To convey clear meaning, it is crucial to establish brightness and color contrast between the *figure* and the *ground*. Additionally, clear color contrast should be present for mapping themes that exhibit *differentiation* relationships, while closely related colors should be used for themes with *association* relationships. Moreover, the color should demonstrate a gradient in terms of saturation and/or brightness for themes with *order* relationships.

Based on these considerations, the denotative quality between two themes can be measured in the CIELab color space using the following approach:

$$f(c_i, c_j, v_{ij}) = \begin{cases} \min\left(1, \frac{\Delta E^*_{ab}(c_i, c_j)}{\delta_t}\right) * \min\left(1, \frac{\Delta L(c_i, c_j)}{\delta_l}\right) & v_{ij} = H \\ \min\left(1, \frac{\Delta E^*_{ab}(c_i, c_j)}{\mu}\right) & v_{ij} = D \\ \min\left(1, \frac{\mu}{\Delta E^*_{ab}(c_i, c_j)}\right) & v_{ij} = A \\ \min\left(1, \frac{\alpha}{\Delta h^*_{ab}(c_i, c_j)}\right) * \min\left(1, \frac{ch^*_{ab\cdot i}}{ch^*_{ab\cdot j}}\right) * \min\left(1, \frac{L_j}{L_i}\right) & v_{ij} = O \\ 0 & i = j \end{cases} \quad (1)$$

where *H*, *D*, *A* and *O* indicate *figure-ground*, *differentiation*, *association,* and *order* relationships, respectively;

*i* and *j* are the indices of any two colors;

$L_i$ and $L_j$ are the color brightnesses of theme *i* and theme *j*;

$c_i$ and $c_j$ are colors of theme *i* and theme *j*;

$h^*_{ab} = \arctan(\frac{b^*}{a^*})$;

$ch^*_{ab}$ is the saturation value;

$ch^*_{ab} = \sqrt{a^2 + b^2}$;

$v_{ij}$ is the intended relationship between two colors;

$\Delta E^*_{ab}$ is the color distance between two colors;

$\Delta h^*_{ab}$ is the tonal difference between two colors;

$\Delta L$ is the brightness distance between two colors;

$\delta_t$ is the color distance threshold for the *figure-ground* relationship;

$\delta_l$ is the brightness distance threshold for the *figure-ground* relationship;

$\mu$ is the color distance threshold for the *differentiation* and *association* relationship;

$\alpha$ is the hue angle threshold for the *order* relationship.

The last four parameters serve as thresholds to determine the effectiveness of encoding these relationships. We assume that the original map is well designed, meaning that its denotative quality is 1. Therefore, the values for these four parameters can be extracted from the original map for further adjustment. By changing the color assigned to a theme, we can measure its impact on denotative quality using this approach. Additionally, as mentioned earlier, elements in both the *figure* and the *ground* can be further semantically distinguished. Hence, the values of $\mu$ and $\alpha$ can be further refined based on the discriminability threshold for semantic relationships in the *figure* and the *ground*.

To measure all the relationships in a map, we create a relationship matrix, denoted as *R*, which is an $n \times n$ matrix, where *n* represents the number of themes. The overall denotative quality can be calculated by summing all the elements in the relationship matrix. To standardize the score, we normalize it to a range from 0 to 1, as follows:

$$Q(C) = \frac{\sum_{i=1}^{n} \sum_{j=1}^{n} f(c_i, c_j, v_{ij})}{n * (n-1)} \qquad (2)$$

where all variables follow the definitions given above.

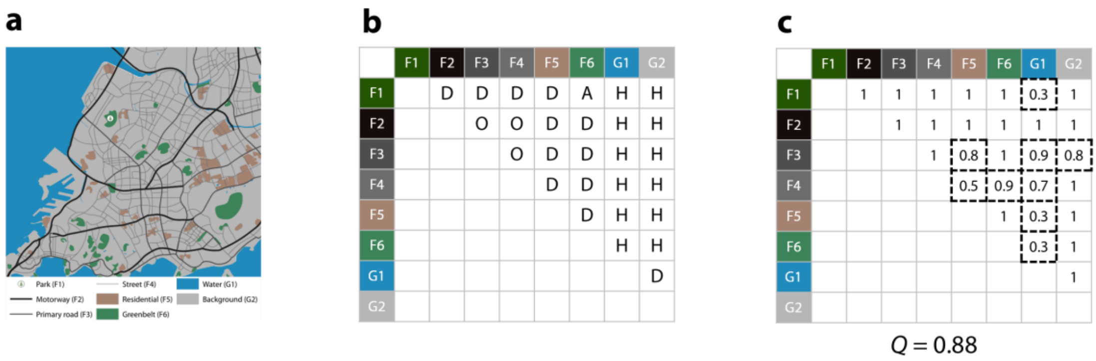


Fig. S5. Example of quantifying a map's denotative quality. **a**, Adjusted map from the example map in Fig. S4a. **b**, Corresponding relationship matrix. **c**, Quantified denotative quality of the adjusted map.

We demonstrate the dimming of the sample map in Fig. S4a by slightly modifying the color scheme, creating an illustrative energy-saving map (see Fig. S5a). The corresponding relationship matrix is depicted in Fig. S5b. As shown in Fig. S5c, after dimming the colors, while the denotative quality of some relationships is preserved (e.g., *order* between motorway and primary road, $f(c_{F1}, c_{F2}, O) = 1$), several relationships are partially distorted (e.g., *differentiation* between street and residential, $f(c_{F4}, c_{F5}, D) = 0.5$). Overall, the adjusted map receives a denotative quality score of 0.88. This method accounts for all possible relationships between any two themes, making it applicable even if the relationships are altered, such as de-emphasizing streets as *ground* or emphasizing water as a *figure*.

### *3.3 Step 2: Energy saving with consideration of figure-ground and semantic relationships*

#### *3.3.1 Organizing a map's denotative quality and energy consumption*

The energy-saving problem for the map involves two objective considerations:

denotative quality and map display energy consumption. To align with the 0-1 range of denotative quality and facilitate problem solving, we convert the absolute map display energy consumption into an energy reduction level ranging from 0 to 1. Consequently, the energy-saving problem can be mathematically formulated as a MAX-MAX problem, represented as follows:

$$\begin{cases} \max Q(C) \\ \max \left(1 - \dfrac{E_n(C)}{E_o(C)}\right) \end{cases} \tag{3}$$

where $Q(C)$ is the denotative quality of the adjusted map;

$E_n(C)$ is the energy consumption of the adjusted map;

$E_o(C)$ is the energy consumption of the original map.

*3.3.2 Local searching for serious energy-saving maps*

We employ a heuristic search method to solve the aforementioned dual-objective optimization problem. Various multi-objective optimization algorithms can be considered, such as the multi-objective artificial bee colony algorithm, multi-objective particle swarm optimization algorithm, and nondominated sorting genetic algorithm-II (NSGA-II). In this study, we choose the NSGA-II algorithm due to its advantages in ensuring solution diversity and effectively covering the solution space of multi-objective functions in the search space. The NSGA-II algorithm operates as follows: first, initialize a set of populations representing potential solutions; second, calculate *fitness* (standing for how good the solution is) of each population and rank the populations using nondominated sorting; then, update populations through operations such as selection, crossover, and mutation; finally, check if the termination conditions are met, which could be reaching the maximum number of iterations or finding a satisfactory solution; if not, repeat steps two and three.

In our case, a population represents a color scheme that includes all the colors used in the maps. We initialize the populations with colors extracted from the original maps. If a population's scores for both objective functions are not inferior to those of other populations and at least one of the objective function results is better than that of other populations, it is considered a nondominated solution. We adjust colors in the HSV color space through multiple iterations of crossover, selection, and mutation on the populations, guided by energy consumption and denotative quality in terms of *fitness*. The set of nondominated populations with the highest *fitness* is known as the *Pareto frontier* solution set.

Since our map energy-saving model incorporates the energy reduction level as one of the objective functions (horizontal axis in Fig. S6a), we can gradually obtain energy-saving maps by regularly sampling the *Pareto frontier*. Using the example map in Fig. S4a as the original map, we sample the optimal solutions at 10%, 20%, 30%, and 40% reduction levels (Fig. S6a), resulting in four energy-gradually reduced maps (Fig. S6b).

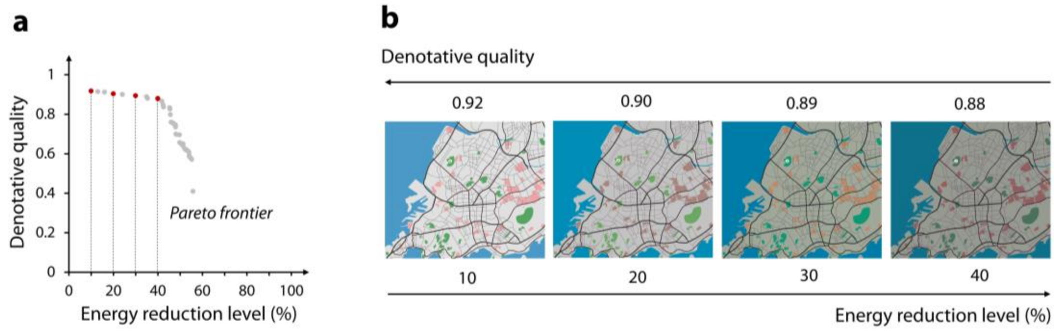


Fig. S6. The result of gradually searching for energy-saving maps. **a**, *Pareto frontier* indicating optimums. **b**, Four energy-saving maps at different energy reduction levels (10%, 20%, 30%, and 40%).

### *3.3.3 Global search with reversed figure-ground initiation to maximize energy-saving*

The local search approach addresses two challenges in identifying energy-minimized maps. First, energy-minimized maps can significantly differ visually from the original maps, making it time-consuming to reach the energy-minimized solution through iterative search. Second, color hue constraints must be carefully considered during map adjustments, as certain hues may have semantic associations (e.g., blue for water). Incorporating color hue constraints would increase the algorithm's complexity. To effectively find the energy-minimized maps, we propose a modification in the initialization phase by reversing the brightness and saturation of each map color. The modified initialization can be represented as:

$$\forall c_i \in C, L_i' = 100 - L_i \ \ and \ \ {ch^*_{ab\cdot i}}' = 100 - \ ch^*_{ab\cdot i} \qquad (4)$$

where $L_i'$ is the adjusted brightness of theme $i$ and ${ch^*_{ab\cdot i}}'$ is the adjusted saturation of theme $i$. In this manner, the solution effectively converges toward the far end of the horizontal axis, representing a high energy reduction level. However, we do not treat the farthest end as the energy-minimized map because it may result in a significant loss of denotative quality. Instead, we aim to explore the *Pareto frontier* to identify a break point that signifies a solution with a maximized energy reduction while minimizing the loss of denotative quality. In practice, when using color to encode *figure-ground* and semantic relationships, the thresholds on color distance are slightly relaxed. As a result, minor color changes may not initially damage the denotative quality. However, once these thresholds are surpassed, even slight color variations can have a cumulative impact on all related themes, leading to a sharp decline in denotative quality. Therefore, the *Pareto frontier* tends to exhibit a convex function form. We consider the point at which the ratio of quality and energy reduction abruptly changes as the energy-minimized maps, striking a compromise between denotative quality and energy reduction.

Taking the map in Fig. S4a as an example, Fig. S7a illustrates the *Pareto frontier* using the reversed *figure-ground* initialization. Fig. S7b shows the solution with reversed brightness and saturation. Fig. S7c displays the solution at the farthest end of the energy reduction axis, marked as a red dot, with a 94% energy reduction. However, its denotative quality is low (0.67). Fig. S7d represents the compromise solution, marked as a blue dot, with an 87% energy reduction, which is considered the energy-minimized solution. Although its energy reduction is lower than that of the farthest end solution (0.90 vs. 1.90 μW/pixel, 94% vs. 87%), its denotative quality is significantly higher (0.98 vs. 0.67).

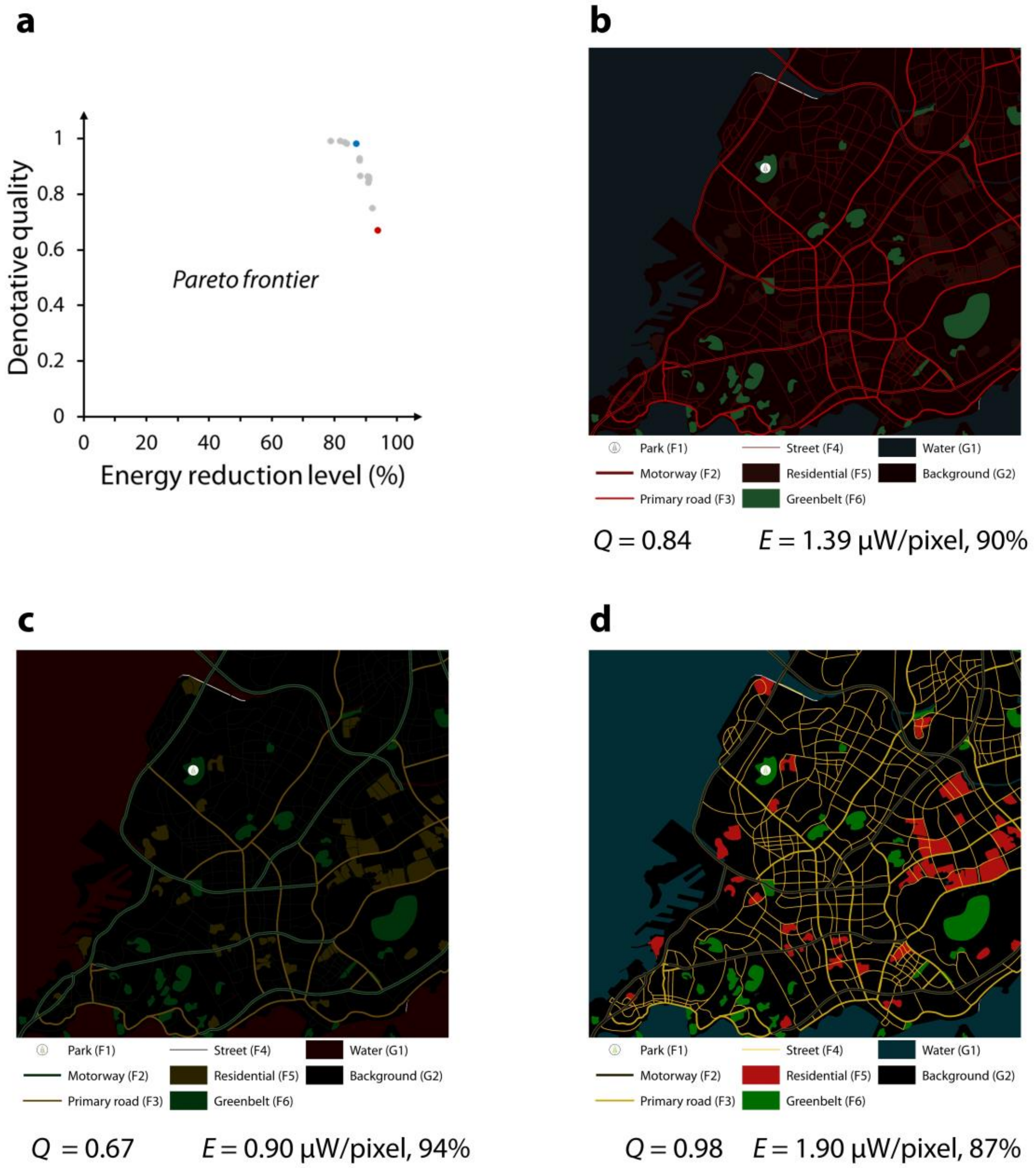


Fig. S7. The result of maximizing energy savings using reversed *figure-ground* initialization. **a**, *Pareto frontier* indicating the optimum. **b**, Reversed brightness and saturation solution for effective searching. **c**, Solution at the farthest end of the energy reduction axis with 94% energy reduction. **d**, Compromise solution with 87% energy reduction.

## 4. Detailed Evaluation Description

To examine the extent to which energy can be reduced without compromising the denotative quality of the original maps, we designed a map-reading experiment.

### 4.1 Materials

We purposely selected four test maps to assess our method (Fig. S8a). By extracting parameters from the original maps (such as $\delta_t$=22, $\delta_l$=10, $\mu$=40, and $\alpha$=10 on Map B; see section 3.2.2 for a discussion of these four parameters), our method can be initialized. We empirically set the population size to 300 and set the number of iterations to 6000 (see section 3.3.2 for a discussion of these two parameters).

Since a 15% energy-saving target is set by The Climate Group (2008) for ICT, we select 15% as a baseline for energy reduction. By employing our gradual search strategy, adjusted maps can be generated at different energy reduction levels, specifically 15%, 30%, and 45% (refer to Fig. S8b).

Utilizing our reversed *figure-ground* searching strategy, we successfully obtain four energy-minimized maps, as illustrated in Fig. S8c. These maps demonstrate a significant reduction in energy consumption, with energy reductions of 91%, 83%, 80%, and 85%. Furthermore, we evaluate the denotative quality of these maps, resulting in values of 0.98, 0.99, 0.94, and 0.89, respectively.

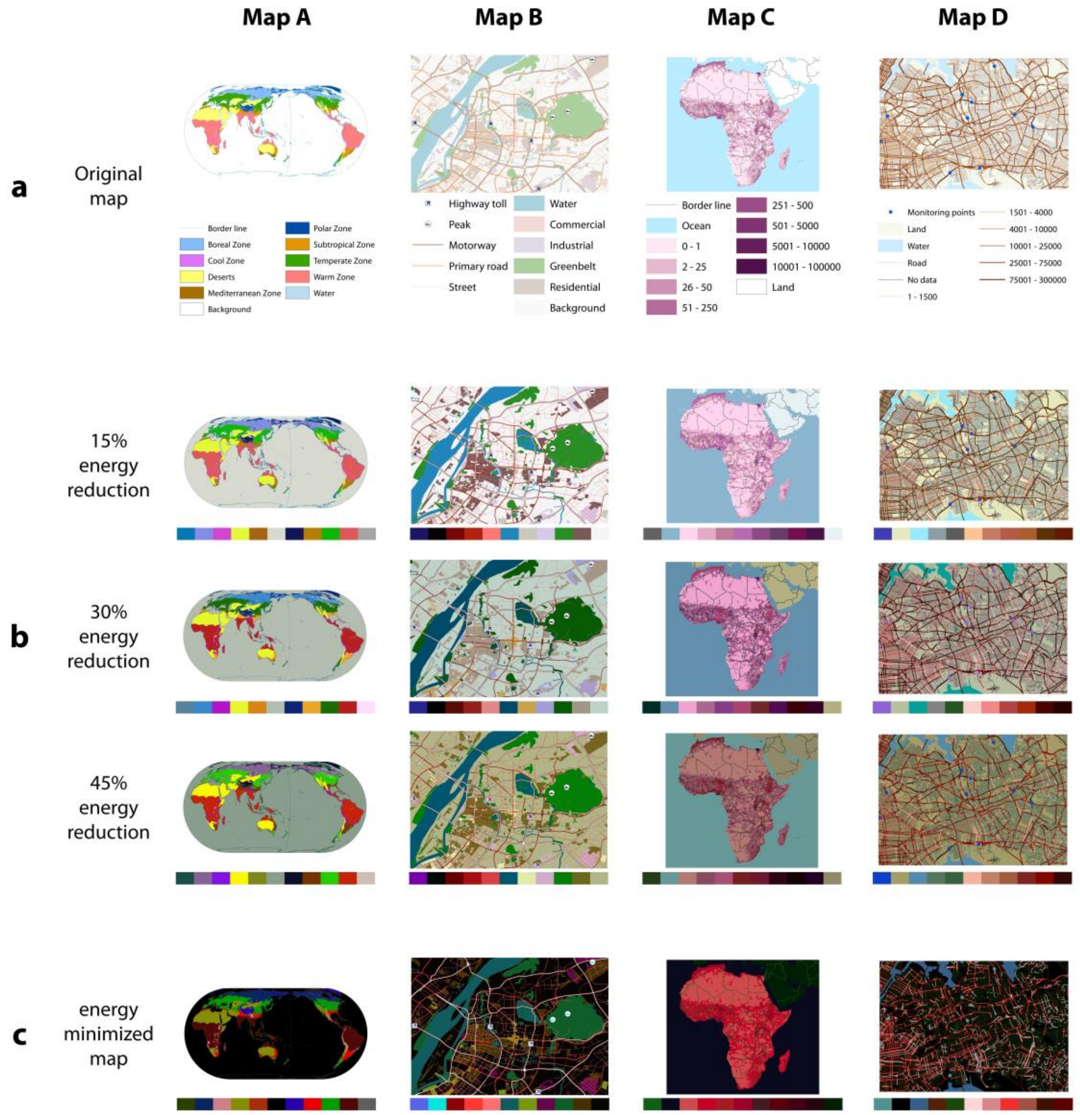


Fig. S8. Test results. **a**, The four original maps. **b**, The results of adjusted maps at 15%, 30% and 45% levels of energy reduction. **c**, Results of four energy minimized maps using our reversed *figure-ground* searching strategy with energy reductions of 91%, 83%, 80%, and 85%.

### *4.2 Participants and procedure*

To assess the denotative quality of the maps at different energy-saving levels, we conducted a map-reading experiment. We recruited 127 volunteer students from the first author’s university to participate in the experiment, excluding those who were already familiar with the test maps. Before the test, we administered a color vision deficiency (CVD) test using 12 Ishihara plates to all participants. Two participants with eye disorders, including weak color vision, who did not pass the test were excluded from the study. Ultimately, we recruited a total of 125 participants, consisting of 60 females and 65 males, ranging in age from 21 to 28 years. By excluding individuals already familiar with the test maps and accounting for potential color vision deficiencies, we aimed to minimize confounding factors and ensure the reliability of our results. All participants provided informed consent, and the protocol was reviewed and approved by the university’s institutional review board.

For the map-reading experiment, we divided the 125 participants into five groups, with each group consisting of 25 participants. Each group was assigned to evaluate a specific version of the maps: the original map and the adjusted maps at 15%, 30% and 45% energy reduction. During the experiment, participants were presented with four test maps and were given three sets of tasks to perform: *identify, locate,* and *compare*. For the *identify* task, participants were randomly given three features to *identify* their types (e.g., "What is the type of feature A?"). In the *locate* task, two areas were randomly selected, and participants were asked to find the location of a specific feature within the chosen area (e.g., "Where is the 'Greenbelt' in area A?"). For the *compare* task, three features were randomly selected, and participants were asked to assess the sortable or ordinal difference between two features (e.g., "Between road A and road B, which road has a higher level?"). To ensure variation and minimize bias, different participants were assigned the same map areas and map features for their tasks at different energy reduction levels. All questions were presented in multiple-choice format, with only one correct answer. Participants were provided with an answer sheet to record their responses, filling in one answer for each question.

To ensure consistency and minimize potential color distortions caused by variations in display screens, we conducted the entire experiment using a single desktop computer equipped with an OLED screen. The screen had a resolution of 1,920 $\times$ 1,080 pixels. Before the experiment, we calibrated the screen to ensure accurate color representation. The calibrated screen was then placed in a quiet laboratory setting with an ambient illumination level of 33.48 candela per square meter ($cd/m^2$). This ambient illumination level corresponds to a normal indoor lighting environment.

Prior to conducting the experiment, we delivered a concise explanation of the experimental process and the equipment used. Subsequently, each participant assumed a comfortable seated position and commenced the task completion process. Upon finishing a set of tasks, participants clicked the mouse to proceed to the next set until all sets of tasks were completed. Overall, it took approximately 10 to 20 minutes for participants to complete the 12 sets of tasks, which were performed on the four test maps. As a token of appreciation for their participation, each participant received a blind box with an approximate value of 10 RMB.

### *4.3 Results and analysis*

In our analysis of the participants' performance, we evaluated two key metrics, effectiveness and efficiency, for both the original maps and the energy-saving maps.

**Effectiveness.** We calculated effectiveness as the average percentage of correctly answered questions for each set of tasks across all participants. To compare the effectiveness of the energy-saving maps with the original maps, we normalized the effectiveness of the energy-saving maps using the effectiveness of the original maps as baseline. As a result, the effectiveness of the original map is considered 1, and higher values indicate better effectiveness for the adjusted maps.

Based on the findings presented in Fig. S9, maps at 15% and 30% energy reduction levels did not exhibit any significant difference in effectiveness compared to the original maps ($p$-value $\geqslant$ 0.05). However, in Map A, one of three sets of tasks at 45% energy reduction showed statistical significance ($p$-value < 0.05), which is consistent with the observations in Map C. For Map B, two of three sets of tasks at 45% energy reduction exhibited statistical significance ($p$-value < 0.05). In the case of Map D, there were no significant differences in any sets of tasks at 45% energy reduction ($p$-value < 0.05).

**Efficiency.** Efficiency was measured by calculating the average time taken (recorded in seconds) to complete a set of tasks by all participants. We normalized the efficiency of the energy-saving maps based on the time usage of the original maps as baselines. Specifically, we divided the time usage on the original map by the time usage on the energy-saving map to determine the efficiency of the energy-saving maps. In this normalization approach, the efficiency of the original map is considered 1, and higher values indicate better efficiency for the adjusted maps.

According to the findings presented in Fig. S9, for all test maps, there were no significant differences in effectiveness between the maps at 15% and 30% energy reduction levels compared to the original maps ($p$-value $\geqslant$ 0.05). However, in the case of Map A, two of three sets of tasks at 45% energy reduction showed statistical significance ($p$-value < 0.05). The same pattern of statistical significance was observed in Map B and Map D. In Map C, all sets of tasks at 45% energy reduction exhibited statistical significance ($p$-value < 0.05).

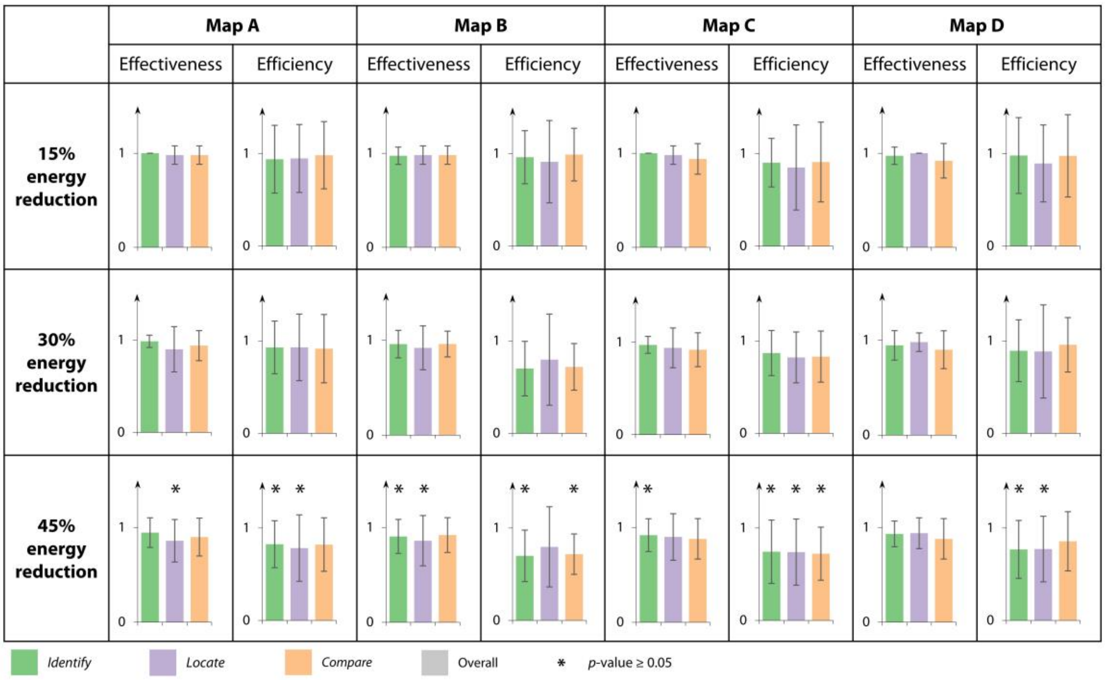


Fig. S9. Statistics of the performance of energy-saving maps at four energy reduction levels for three groups of map-reading tasks (*locate*, *identify*, and *compare*).

When comparing the results of effectiveness and efficiency across different levels of energy reduction, it becomes apparent that the denotative quality of the maps is compromised to varying degrees, as our method considers both denotative quality and map display energy consumption. This compromise is achieved through heuristic map adjustment. When making slight color changes to the maps, the effectiveness and efficiency of map reading may not be directly affected due to the preservation of color proximity and contrast, despite the lower denotative quality. However, significant color changes, especially in terms of color hue and/or brightness contrast, are likely to impact the effectiveness and efficiency. As depicted in Fig. S8, when the energy reduction level reaches 45%, although a relatively clear *figure-ground* relationship can still be maintained, the color brightness contrast between the *figures* and the *grounds* diminishes compared to the results at 15% and 30% reduction levels. Furthermore, the maintenance of semantic relationships between map features is disrupted, which may have a negative impact on effectiveness and efficiency. Analyzing the statistical results of effectiveness and efficiency, we observe that compared to the original map, there is a higher number of task sets that demonstrate significance in terms of efficiency rather than effectiveness. This suggests that even though participants can correctly complete some map-reading tasks, it requires a considerable amount of time, ultimately reducing the overall efficiency of map utilization.

In addition to separately analyzing the effectiveness and efficiency of different maps, we conducted an overall performance analysis by combining the results of effectiveness and efficiency across all four test maps (as shown in Fig. S10). The statistical findings indicate that, in general, maps at 15% and 30% energy reduction levels exhibit no significant difference compared to the original map ($p$-value $\geqslant$ 0.05). However, maps at the 45% energy reduction level show a slight difference.

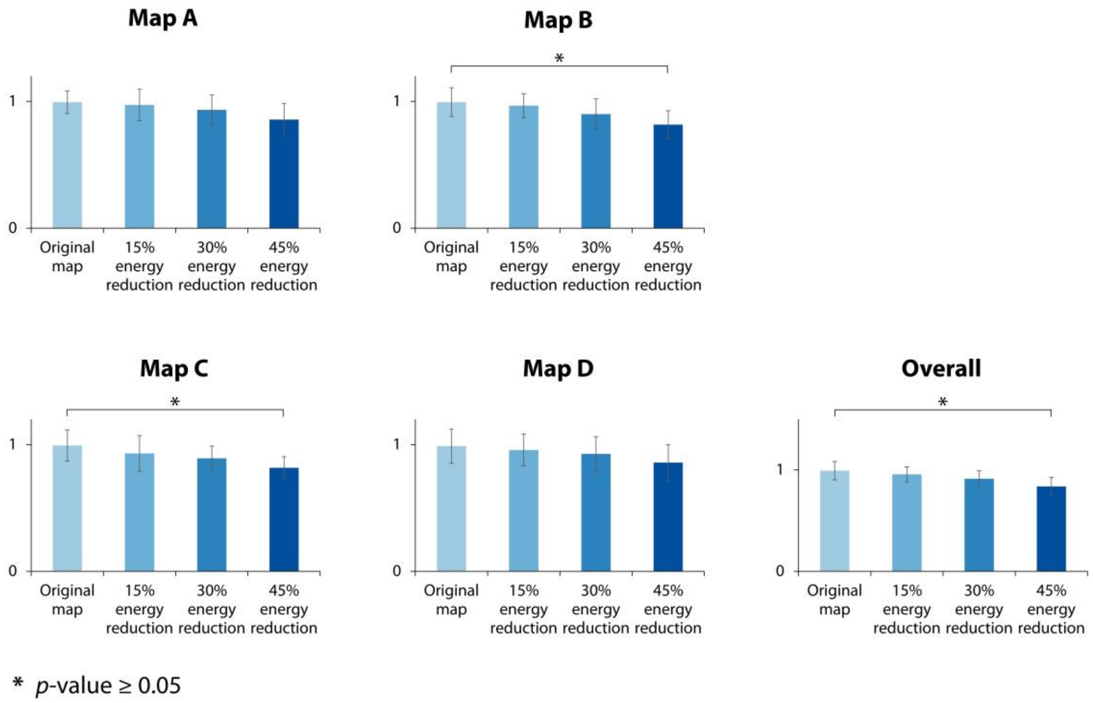


Fig. S10. Overall statistics of the performance of energy-saving maps at four energy reduction levels on three groups of map-reading tasks with the performance of the original maps used as the baseline.

Based on these results, we conclude that our method can achieve a map display energy reduction of up to 30%. This outcome surpasses the 15% energy-saving target set by The Climate Group (2008) for ICT, thereby demonstrating the effectiveness of our approach in significantly reducing energy consumption while maintaining a reasonable level of map usability.